JOURNAL OF GEOPHYSICAL RESEARCH, VOL. 92, NO. B5, PAGES 3597–3602, APRIL 10, 1987

Nonlinear Generation of Elastic Waves in Crystalline Rock

PAUL A. JOHNSON AND THOMAS J. SHANKLAND

Earth and Space Sciences Division, Los Alamos National Laboratory, Los Alamos, New Mexico

RICHARD J. O'CONNELL

Department of Earth and Planetary Sciences, Harvard University, Cambridge, Massachusetts

JAMES N. ALBRIGHT

Earth and Space Sciences Division, Los Alamos National Laboratory, Los Alamos, New Mexico

The nonlinear interaction of two elastic waves at frequencies f_1 and f_2 in an elastically nonlinear material can give rise to a collimated wave at the difference frequency $f_1 - f_2$. Because the amplitude of a difference frequency beam is proportional to the degree of elastic nonlinearity of the material through which it passes, amplitude should be higher in a material containing microcracks such as rock than it is in uncracked materials such as metals, single crystals, or water in which nonlinear elastic interactions have previously been observed. The "nonlinear signal" is important for investigating the nonlinear properties of rocks. Such a beam has already proved useful as a low-frequency acoustic source in water and may ultimately be useful in geophysical exploration. In this paper, our observations of nonlinear signal generation in experiments with crystalline rocks are presented. Three criteria must be fulfilled in such experiments to establish that nonlinear interactions take place in the rock and not in the associated experimental apparatus: (1) The frequency of the observed nonlinear signal must precisely equal the difference frequency $\Delta f = f_1 - f_2$, (2) the amplitude of the nonlinear signal must be proportional to the product of the amplitudes of the primary beams, and (3) the trajectory of the nonlinear signal, which is a function of the input trajectories, wave types, frequencies, and rock velocities, must match that predicted by theory. We observed signals that satisfy the above three criteria in the frequency range from 0.1 to 1.0 MHz.

INTRODUCTION

Nonlinear elastic properties and their effects have received considerable study in the field of acoustics. *Westervelt* [1963] showed that two near-source, collinear (i.e., parallel), high-frequency "carrier" waves could interact to produce sound with frequencies equal to the sum and difference of the high-frequency carriers while retaining a radiation pattern characteristic of the carriers. The radiation pattern, formed when two monochromatic collinear carriers were injected into an elastically nonlinear medium, was shown to be similar to the pattern caused by a long linear array of signal sources in the medium itself. The collinear configuration has been called an end fire or parametric array by *Bellin and Beyer* [1962], who produced evidence showing parametric array formation in water-filled tanks and in air. *Muir and Willette* [1972] demonstrated that the far-field radiation pattern of the beams at the sum and difference frequencies created by a parametric array was narrow and had no side lobes. *Unterberger et al.* [1981] conducted experiments of parametric array formation in a salt dome. The signal at the difference frequency Δf is of particular interest since its amplitude decays more slowly with distance because of its longer wavelength. Thus despite the fact that the energy conversion from the primary input beams to the difference frequency beam is inefficient [*Taylor and Rollins*, 1964], the combined effects of collimation and lower spatial attenuation produce a useful low-frequency acoustic source; exploitation of nonlinear beam generation has led to development of new technologies in echo sounding [*Nichols*, 1971], underwater communications, and probing of shallow sediments beneath water [*Muir*, 1976].

In experiments by other workers, the acoustic medium has been a uniform, uncracked material such as water, salt, metal, glass, or single crystals in which the nonlinearity arises primarily from the nonlinear elasticity of the material itself [*Hiki and Mukai*, 1973]. We have used rocks, which are inherently much more nonlinear than the above mentioned materials, because rocks contain numerous microcracks that give rise to large changes of velocity with pressure [*Birch*, 1960]. In geophysics, elastic nonlinearity has usually been studied in connection with equations of state in which nonlinear contributions appear as third-order or higher terms in the elastic free energy expansion. These higher-order contributions are much greater in microcracked material [*Watt et al.*, 1976]. Since the amplitude of the nonlinear signal is proportional to the value of the higher-order terms [*Hiki and Mukai*, 1973], the larger nonlinear terms in microcracked material should be reflected in a larger amplitude of the difference frequency beam. Therefore, using rocks in nonlinear experiments should enhance the amplitude of the difference frequency beam as compared with the amplitude generated in uncracked materials. Eventually, we hope to study the nonlinearity of rocks through experimental observations of the difference frequency beam amplitude. Such studies could show how effective bulk and shear moduli vary with pressure.

In presenting experimental observations of the nonlinear interaction of elastic waves in crystalline rocks, a necessary first step is to confirm that the observed nonlinearity occurs within the bulk of the rock rather than in associated electronic apparatus. Our work has taken two principal directions as a

Paper number 6B6260.
0148-0227/87/006B-6260$05.00

result. First, we have investigated a number of different sample geometries, configurations of acoustic drivers and receivers, and electronic driving and detection methods in order to produce measurable, verifiable nonlinear effects. The two experimental geometries include (1) those that employ the collinear mixing of beams and (2) those of a noncollinear type in which two beams intersect at a predetermined angle. From these measurements the difference frequency beam, which propagates in a theoretically prescribed direction from the primary beams, is detected. Second, we have varied the experimental conditions so that nonlinear signals arising from wave interactions inside the rock samples can be differentiated from those that might arise elsewhere (within amplifiers and transducers or from surface wave interaction on the sample itself). We use the terms "nonlinear signal," "difference frequency signal," and "Δf signal" synonymously throughout the following discussion.

OBSERVATION OF COLLINEAR MIXING

Several criteria must be met to determine the origin of a nonlinear signal and verify that it arises from nonlinear effects in the rock. The first criterion is, of course, that the frequency of the detected nonlinear signal should equal $f_1 - f_2$. Accordingly, we searched for a signal at the difference frequency that occurred when the frequencies of the driving transducers were varied. A second criterion is that the amplitude of the difference frequency beam $A_{\Delta f}$ should be proportional to the product of the amplitudes of the driving signals [*Jones and Kobett*, 1963; *Rolleigh*, 1975]. Because these two tests did not necessarily distinguish between nonlinear signals originating in the rock and those produced in the external transducers and electronics or through surface wave interaction, we also checked for directional effects. That is, when two collinear beams interact in the rock, the difference frequency beam should have a degree of collimation approximating that of the driving beams [*Welsby*, 1970; *Rolleigh*, 1975]. Hence our third criterion was directionality of the difference beam.

Figure 1 is a diagram of the test apparatus used to verify

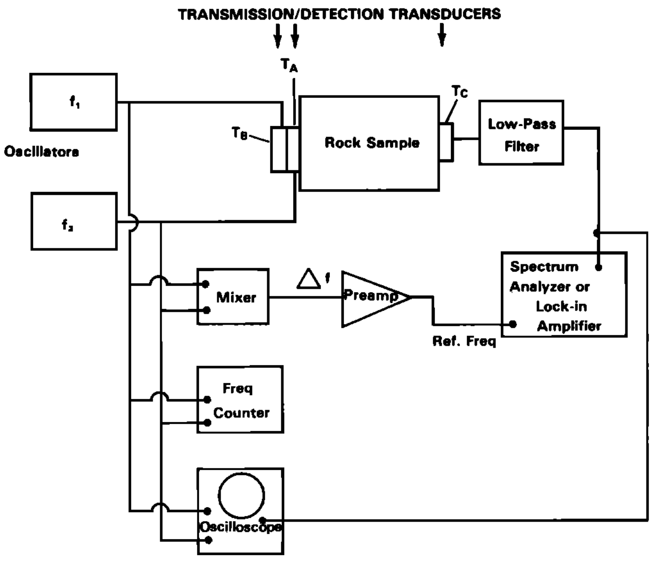

Fig. 1. Configuration for collinear parametric experiments. For a given experiment, any two of transducers T_A, T_B, or T_C were used as drivers, while the third transducer was used as a detector. In all cases, two compressional wave inputs produce a compressional wave at the difference frequency.

TABLE 1. Average Rock Velocities

	v_p, km/s	v_s, km/s
Berkeley blue granite	3.33	2.26
Starlight Black quartz norite	5.67	3.39

the first criterion. We initially used Berkeley blue granite (Elberton, Georgia) for these experiments. The 112-mm-long by 54-mm-wide sample had piezoelectric (PZT) compressional wave transducers T_A and T_B at one end and a third compressional wave transducer T_C at the other. The transducers were coupled to the rock with vacuum grease. Average compressional and shear wave velocities for this rock are 3.33 and 2.26 km/s, respectively, as shown in Table 1. In these experiments, typical wavelengths were about 3–5 mm; since the transducer diameters were either 25 or 40 mm and thus several wavelengths wide, the resulting beams were reasonably well collimated. Grain sizes are about 1 mm, well below typical wavelengths. When we drove T_A at 1113.81 kHz and T_B at 1178.51 kHz, we observed a difference frequency of 64.6 kHz at T_C with a Nicolet 660A Fast Fourier transform (FFT) frequency analyzer. In fact, using the FFT frequency analyzer, we observed that the difference frequency response indeed tracked the value of $f_1 - f_2$ when either f_1 or f_2 was independently swept over a broad frequency range.

Using the same experimental configuration, we verified the second criterion: The amplitude of the difference frequency signal $A_{\Delta f}$ should be proportional to the product of the amplitudes of the two primary beams A_1 and A_2. Figure 2 shows the results of the experiment, which demonstrate the linear relation between the observed input and output amplitudes; A_1 and A_2 were varied independently, and the received amplitudes were plotted against the product of the amplitudes applied to the rock. Because we suspected a nonlinear signal originating in the driving transducers T_A and T_B, we checked these results using a second configuration in which the driving transducers were placed at opposite sides of the sample (T_B and T_C in Figure 1), and signals were detected with T_A. In this case, if the mixing were taking place inside the rock sample, most of the mixing should have occurred near the center of the sample. Therefore, if the signal originated in the rock, the amplitude of the difference frequency signal should approximately reflect the amplitude losses of the primary beams traveling to the rock center and the difference frequency beam traveling from the rock center to the detecting transducer ($A_{\Delta f}$ is proportional to A_1 times A_2). However, if the nonlinear signal arose from mixing in the transducer, its amplitude should be decreased by about the same amount of loss suffered by the primary beam across the sample because the input signal from T_C must first traverse the rock before interacting with T_B. The primary beam amplitude loss across the sample was about 34 dB. The observed difference frequency signal, however, was only about 4 dB lower than that in the first case, thus demonstrating that the detected Δf signal originated in the rock. This experiment also excluded the possibility that the nonlinear signal was created in the associated electronics and was beamed into the sample. That is, if the difference frequency had been produced in the electronics, attenuating would have caused a larger signal to occur when the detecting and driving transducers were face to face than when the detector and driver were at opposite ends of the rock. In fact, the opposite observation was made, which indicates that

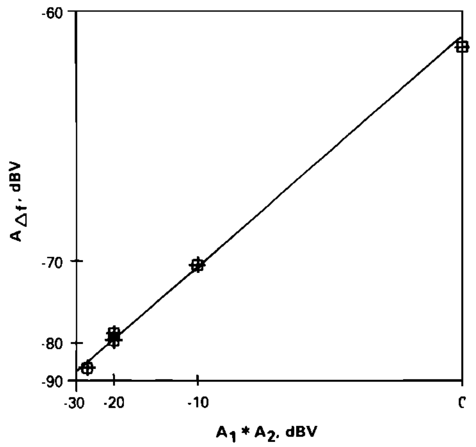

Fig. 2. Linear dependence of the amplitude of Δf on the product of the input amplitudes. Accuracy of measurements is better than ± 2 dB V.

the nonlinear signal was produced in the rock and not in the associated electronics. The oscillators driving T_B and T_C were switched in this configuration to be certain that neither was transmitting an electronically produced nonlinear signal.

As a further test of the amplitude proportionality criterion, we conducted another experiment to measure signal intensities using an Ithaco 393 lock-in analyzer in place of the spectrum analyzer shown in the Figure 1 configuration. Two oscillators produced primary frequencies f_1 and f_2 at T_A and T_B; f_1, f_2, and Δf across the rock were detected with a third transducer T_C. A frequency counter supplied exact values of frequencies, and the lock-in amplifier was used as a narrow-band detector precisely at the difference frequency. The reference frequency for the lock-in amplifier was supplied by mixing the primary frequencies using a separate mixer and preamplifier. As a representative case, using signals $f_1 = 480.28$ kHz and $f_2 = 536.77$ kHz ($f_2 - f_1 = 56.49$ kHz), we obtained the received amplitude ratio $A_\Delta f$(peak-peak)/[$A_1 + A_2$(peak-peak)] = 3.1×10^{-3}. At these amplitude levels it was necessary to check any nonlinear contributions arising from intermodulation within the lock-in amplifier. The ratio of the intermodulation to the sum of the received primary amplitudes was separately measured to be 0.17×10^{-3}, only 6% of the ratio measured at the receiver transducer. As expected, when a long sample (406 x 90 x 90 mm) was used, the primary beams were more attenuated than the difference beam, and the amplitude ratio rose to 11.5×10^{-3}. The amplitude ratio increased because the difference frequency beam was lower in frequency and thus attenuated less rapidly. To test the amplitude proportionality criterion using this sample, we inserted a 10-dB attenuator between the power amplifiers and the f_1 transducer, which reduced the amplitude of the Δf signal level by about 10 dB. Inserting a second 10-dB attenuator into channel 2 gave a further drop of 10 dB, thus fulfilling the criterion.

Tests of the third criterion, directionality, for which we used the collinear configuration shown in Figure 1, were more difficult. Reflections of both primary and difference frequency beams from the sample walls affected beam width, and contacts between the detector-transducer and the rock were difficult to reproduce. Contact reproducibility is important because the Δf beam amplitude must be measured at several points away from the theoretically predicted angle of peak amplitude. If the contacts are not reproducible, this measurement could be inconclusive. Therefore, to test the third criterion, we carried out a second set of experiments using noncollinear geometries.

NONCOLLINEAR BEAM MIXING MEASUREMENTS

In this section we provide evidence that the nonlinear interaction occurs within the rock by demonstrating that certain selection rules governing the nonlinear interactions are obeyed. *Jones and Kobett* [1963] and *Taylor and Rollins* [1964] derived the nonlinear wave equation and determined selection rules for the general case of two collimated, monochromatic plane wave beams interacting at arbitrary angles in a homogeneous isotropic material. Five possible interactions exist between P and P, S and S, or S and P waves that produce a wave at either a difference or a sum frequency. Table 2 lists the selection rules for the two cases relevant to this work, which are two longitudinal primary waves producing a transverse wave at the difference frequency and a longitudinal and transverse primary wave producing a longitudinal wave at the difference frequency.

The selection rules define the permissible interaction geometry for the generation of a nonlinear difference frequency signal at a given frequency ratio f_2/f_1 and at given wave speeds v_p/v_s. Once two frequencies are chosen for a material with known v_p/v_s, the input and output angles required for the formation of the nonlinear beam are prescribed. The finite beam width, however, permits an angular range over which the output beam can be detected. A graphical representation derived from the selection rules for two input compressional waves is shown in Figure 3 for a sample with $v_p/v_s = 1.67$. As an example, if the two primary frequencies are 1000 and 610 kHz, respectively, then the angle between the primary beams

TABLE 2. Selection Rules for Two Interaction Cases

Interaction	$\cos\phi$	$\tan\gamma$	Plane of S Wave Polarization
$P(\omega_1) + P(\omega_2) \rightarrow S(\omega_1 - \omega_2)$	$\dfrac{1}{c^2} - \dfrac{(1-c^2)(a^2+1)}{2ac^2}$	$\dfrac{-a\sin\phi}{1 - a\cos\phi}$	$k_1 - k_2 - k_3$
$P(\omega_1) + S(\omega_2) \rightarrow P(\omega_1 - \omega_2)$	$c + \dfrac{a(1-c^2)}{2c}$	$\dfrac{-a\sin\phi}{c - a\cos\phi}$	$k_1 - k_2 - k_3$

P and S refer to longitudinal and transverse waves, respectively; ω is the angular frequency; ϕ is the angle between k_1 and k_2; and γ is the angle between k_1 and k_3, where k_1, k_2, and k_3 are the propagation directions shown in Figure 4; a is the frequency ratio f_2/f_1; and c is the velocity ratio v_s/v_p. For these two interaction cases, all shear waves are polarized in the plane formed by $k_1 - k_2 - k_3$ [*Taylor and Rollins*, 1964; *Jones and Kobett*, 1963]. Note that case $P + P \rightarrow P$, which is usually used in acoustic applications such as sonar, is collinear.

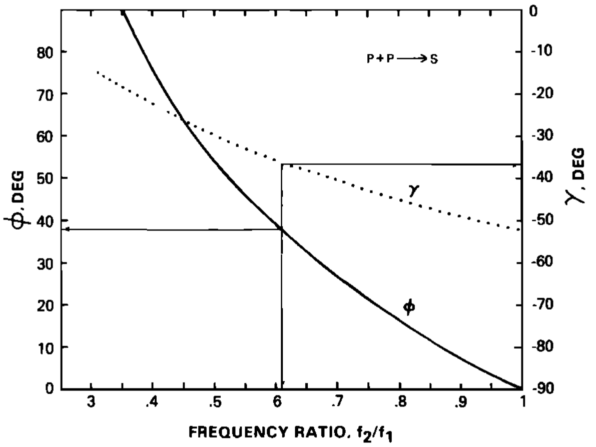

Fig. 3. Curves for the $P + P \rightarrow S$ case derived from the selection rules showing the interdependence of input angle ϕ, output angle γ, and frequency ratio a for $v_p/v_s = 1.67$. Lines show input and output angles for a frequency ratio f_2/f_1 of 0.61. Plan view of beam geometry is shown in Figure 4.

ϕ is 39° and the output angle γ is $-36°$ as shown by the lines in Figure 3. (See Figure 4 for a diagram showing these angles.)

Figure 4 illustrates the experimental configuration used for the general case of intersecting beams. The two primary acoustic inputs were PZT transducers that were independently driven by two separate function generators whose signals were amplified by separate power amplifiers. The function generators produced continuous monochromatic sine waves, and the signal at the difference frequency was detected by a third transducer connected to the spectrum analyzer. The transducer was bonded to the sample with phenyl salicylate. The sample used was "Sealmark Starlight Black" (trademark belonging to the Rock of Ages Company, Barre, Vermont), a quartz norite from Belfast, South Africa. This quartz norite is less anisotropic than Berkeley blue, which has an approximately 37% and 17% P and S wave velocity variation, respectively. Starlight Black had a 5.3% P wave velocity variation and a 5.6% S wave variation in three perpendicular directions about means of 5.67 and 3.39 km/s, respectively (Table 1); the average measured v_p/v_s was 1.67. We used a less anisotropic rock than Berkeley blue in this case because anisotropy tended to enhance beam spreading, thereby complicating the observation. Transducers with fundamental frequencies of 250, 500, and 1000 kHz were used in our experiments, performed at frequencies of 150–1000 kHz.

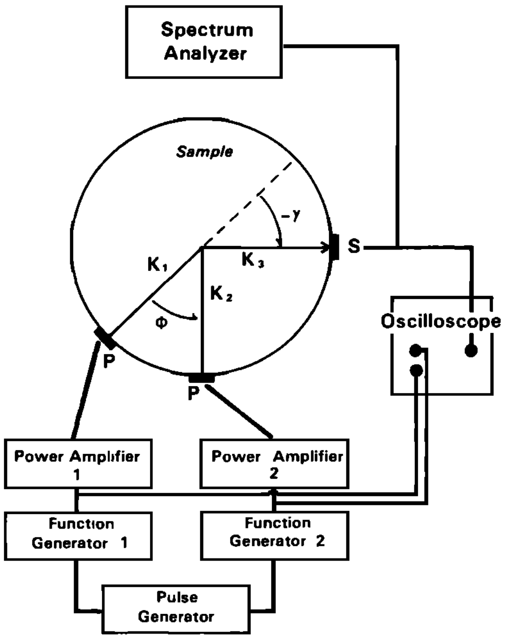

Fig. 4. Block diagram of experimental configuration. The k_1, k_2, and k_3 are wave propagation directions, and ϕ and γ show relationships of the interaction geometry. The P and S refer to compressional and shear waves, respectively.

As in the collinear experiments, there was the possibility that nonlinear interactions could take place within the electronics or, in this experiment, through surface wave interaction between primary transducers and then be transmitted into the rock. We performed experiments to verify that the observed difference frequency was produced in the geometry given by the selection rules, thus demonstrating that the nonlinear interaction originated within the rock. If the difference frequency was created in the electronics or transducers, the spatial dependence predicted by the selection rules would not have been observed.

For the following experiments, we departed from the cylindrical sample geometry and cut the rock specifically for the interaction case $P + P \rightarrow S$, where frequency ratio $a = 0.61$, $\phi = 39°$, and $\gamma = -36°$, and the $P + S \rightarrow P$ case, where $a = 0.36$, $\gamma = 38°$, and $\gamma = -35°$. This sample geometry was used so that the transducers could be attached to planar faces on the rock to improve bonding and bond reproducibility. The sample is shown in the inset of Figure 5, and sample dimensions are noted in the Figure 5 caption. Typical wavelengths are 5–50 mm, much smaller than the sample dimensions, and grain size is again of the order of 1 mm. In the initial experiment, ϕ and γ were 39° and $-36°$, respectively, for two compressional wave sources. These are the angles shown in Figure 3. Figure 3 also shows that the peak amplitude of the wave should occur at $a = f_2/f_1 = 0.61$. Furthermore, as noted in the selection rules (Table 2), the nonlinear signal should be a shear wave polarized in the propagation plane k_1-k_2-k_3 shown in Figure 4. We held f_1 at 610 kHz and constant input voltage, while f_2 (also at constant input voltage) was swept from 220 to 510 kHz. From the selection rules we expected that when f_2 gave the correct frequency ratio of

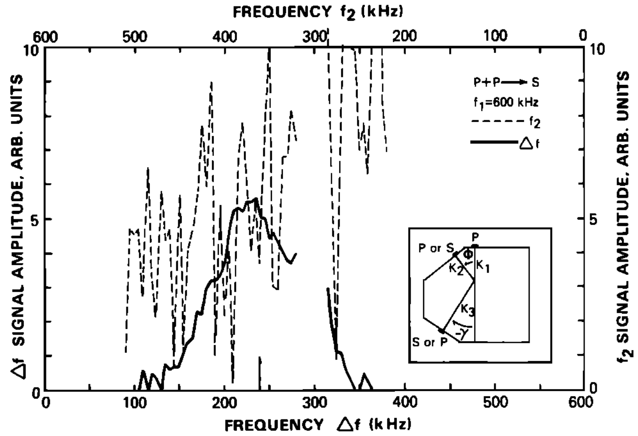

Fig. 5. Linear amplitude dependence of the Δf beam on the change in f_2 (or Δf). Peak amplitude should occur at $a = f_2/f_1 = 0.6$ for the geometry (arrow). The dashed line shows the received amplitude of f_2. The data gap near $\Delta f = 300$ kHz is due to the overlap of f_2 and Δf on the spectrum analyzer. Inset shows the sample geometry used in this and following experiments; sample dimensions are 282 × 284 × 160 mm.

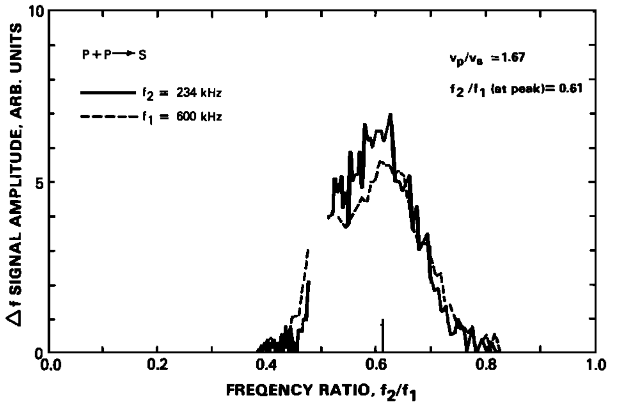

Fig. 6. Frequency ratio dependence of $A_{\Delta f}$: first, sweeping f_2 while f_1 is held constant (solid line); second, sweeping f_1 while f_2 is held constant (dashed line). Peak response at $f_1 = 600$, $f_2 = 366$ kHz, $f_2/f_1 = 0.61$ (arrow). Amplitude units are linear.

0.61 for this geometry, the amplitude of the Δf signal should have been a maximum. As f_2 was increased or decreased away from this ratio, the Δf signal amplitude should have decreased since the selection rules indicate that if the frequency is changed, so must ϕ and γ change for maximum $A_{\Delta f}$. Figure 5 shows the results of this experiment. The output amplitude of both the difference frequency (solid line) and f_2 (dashed line) was recorded at 5-kHz increments through the sweep interval. The maximum amplitude of the Δf signal did indeed occur at $a = 372/610 = 0.61$, $\Delta f = 238$ kHz. Note that the proportionality between the amplitude of the difference frequency signal and the product of the amplitude of the primary beams only holds for the predicted geometry derived through the selection rules. Thus the amplitude of f_2 (dashed line) is independent of the response of the difference frequency signal. In addition, if the difference frequency response had originated from surface wave interaction or intermodulation in electronics, we would have expected the Δf signal response to be proportional to the received amplitude of f_2 rather than to the predicted peak response. The extremely variable f_2 amplitude is due to constructive and destructive interference effects produced by the sample size and geometry, plus the effect of changes between nodal and antinodal position of source and receiver as frequency changes.

We also demonstrated that a similar response was observed when the roles of f_1 and f_2 were reversed. The plot in Figure 6 shows the signal amplitude of the Δf signal versus the frequency ratio for both experiments, i.e., holding f_1 constant and sweeping f_2 (dashed line) and holding f_2 constant and sweeping f_1 (solid line). The results were nearly identical; both peaks in the amplitude of the Δf signal occurred at a frequency ratio of approximately 0.61, and the shapes of the curves match very well, indicating nearly identical amplitude responses in each case. This response could only appear if the difference frequency was produced within the intersection volume of the primary beams in the rock.

As noted, the selection rules state that for a given input angle ϕ or a given output angle γ the frequency ratio for the maximum amplitude of the nonlinear signal is fixed. Therefore, to show that the above observation was independent of frequency as long as the frequency ratio remained constant, we repeated the frequency sweep experiment by holding f_1 at 500 kHz and sweeping f_2, where the frequency ratio a at peak amplitude for this geometry was $305/500 = 0.61$ for the $P + P \rightarrow S$ case. We used the same geometrical configuration

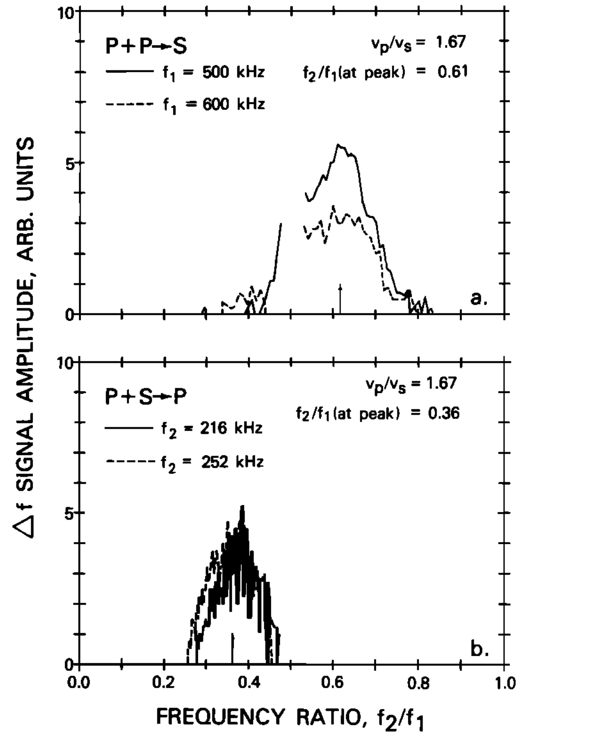

Fig. 7. Frequency dependence of $A_{\Delta f}$ for two interaction cases given in Table 3. Note that each case shows the same dependence on frequency ratio. The $a = f_2/f_1$ is the ratio for which the maximum amplitude of the difference frequency should be obtained (arrows). Amplitude units are linear.

as that used for the preceding experiment. Second, to show that the result was independent of the particular case of wave interaction (as theory predicts), we repeated the experiment for $P + S \rightarrow P$, where $a = 252/700 = 0.36$ at peak $A_{\Delta f}$. Here f_2 was held at 252 kHz, and f_1 was swept between 300 and 1000 kHz. Finally, to again demonstrate the independence of frequency range for a given frequency ratio, for $P + S \rightarrow P$ where $a = 216/600 = 0.36$, we held f_2 at 216 kHz and swept f_1 between 250 and 1000 kHz. For these latter two experiments, ϕ and γ were 38° and −35°, respectively.

Results for the first of these experiments together with results from the initial experiment (Figure 5), are shown in Figure 7*a*; results for the second and third experiments are in Figure 7*b*. Pertinent information for each curve is given in Table 3. Most importantly, Figure 7 indicates that we could exclude the formation of the Δf signal anywhere but in the rock. Otherwise, the peak response of $A_{\Delta f}$ would not have occurred at the predicted frequency ratio a in each of these cases. In addition, as the selection rules predict, the formation of the Δf beam in the rock formed independently of input frequencies for a given frequency ratio and geometry; this result was observed in both interaction cases.

The actual beam width could not be determined from the curves in Figures 5–7. Accordingly, in a further experiment we

TABLE 3. Frequency Dependence of $A_{\Delta f}$ for Two Interaction Cases

Case	a	f_1, kHz	f_2, kHz	Symbol in Figure 7
$P + P \rightarrow S$	0.6	600	swept	solid line, Figure 7*a*
$P + P \rightarrow S$	0.6	500	swept	dashed line, Figure 7*a*
$P + S \rightarrow P$	0.36	swept	252	solid line, Figure 7*b*
$P + S \rightarrow P$	0.36	swept	216	dashed line, Figure 7*b*

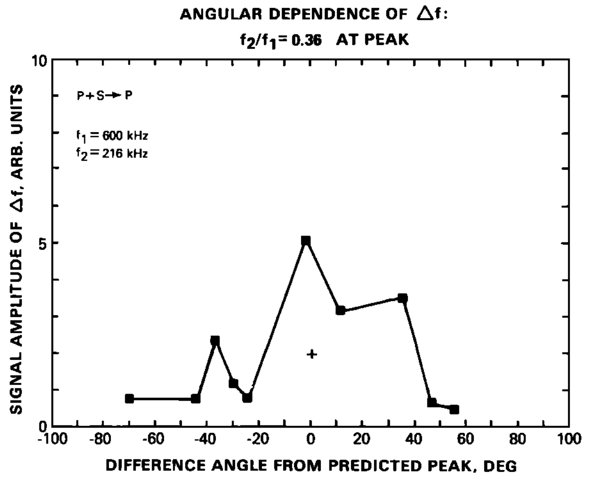

Fig. 8. Angular dependence of the amplitude of Δf measured from the predicted angle of $\gamma = -35°$. The plus indicates amplitude measurement of Δf signal at 90° polarization. Amplitude units are linear.

measured the directionality of the difference frequency wave for the $P + S \rightarrow P$ case by moving the receiving transducer $\pm 60°$ from the calculated angle γ. At each location we observed the amplitude of the Δf signal on the spectrum analyzer.

The angular variation in the observed amplitude response is shown in Figure 8. The difficulty of duplicating transducer bonds is reflected in the roughness of the curve, as are focusing effects from corners in the noncylindrical rock sample, e.g., the points 35° and $-38°$ from the predicted angle γ. Nevertheless, the overall shape of the curve demonstrates the directional dependence of the difference frequency wave and shows qualitatively the beam width of the Δf signal for the $P + S \rightarrow P$ case.

An additional test was made with the configuration shown in Figure 5. Since the polarization direction of the shear wave must be in the plane formed by the wave vectors k_1-k_2-k_3 [*Taylor and Rollins*, 1964], the shear wave input f_2 was polarized in the plane perpendicular to the plane formed by k_1-k_2-k_3 to see if the Δf signal decreased in amplitude. The cross at zero degrees in Figure 8 shows that the measured amplitude of the Δf beam indeed decreased when the f_2 beam was polarized perpendicular to the k_1-k_2-k_3 plane. Although theoretically the difference frequency should not have formed at all in this geometry, other observers have noted the same phenomena in measurements with single crystals [e.g., *Hiki and Mukai*, 1973]. As these workers noted, the shear wave input transducer may not produce a perfectly polarized signal, and in our case, elastic anisotropy could have enhanced the wronglypolarized signal. As a further check of polarization, we found that for $P + P \rightarrow S$, the output shear wave was dominantly polarized in the k_1-k_2-k_3 plane, as predicted.

CONCLUSIONS

We have demonstrated that the nonlinear interaction of two elastic waves creates a wave at the difference frequency in two types of crystalline rock.

1. The difference frequency tracked $f_1 - f_2$ where the primary frequency f_1 or f_2 was swept over a large frequency range.

2. Experiments clearly showed that the amplitude of the difference frequency was proportional to the product of the amplitudes of the primary driving frequencies.

3. The directional dependence of the amplitude of the difference frequency beam was demonstrated in noncollinear experiments by sweeping either f_1 or f_2 away from the correct frequency ratio for computed angles of interaction. In these latter experiments, a peak amplitude in the Δf signal was observed at the expected frequency ratio for the appropriate geometry and interaction case, and the amplitude decreased away from this peak. Furthermore, we observed a decrease in the amplitude of the Δf signal by moving the output transducer away from the theoretically predicted peak while leaving the frequency ratio unchanged.

4. Finally, we observed the predicted polarity dependence of the Δf signal amplitude.

The general conclusion is that nonlinear interaction of elastic waves can occur in a heterogeneous material such as rock and that the strong elastic nonlinearity of such materials may prove useful. For example, the Δf signal may be of use as a seismic source in geophysical exploration applications. Of academic interest is the application of the technique to the study of nonlinear properties of rocks.

Acknowledgments. We are grateful to Gary Luedemann, Evon Stephani, and Ray Jermance for experimental assistance and to Mike Fehler and Scott Phillips for proofreading the manuscript and numerous comments. We wish to thank Fred Rollins, who provided many useful experimental suggestions, and also Jean Butler, Cheryl Straub, Gloria Carlisle, and Ada DeAguero, who typed revisions of the manuscript. This work was supported through George Kolstad, Office of Basic Energy Sciences, U.S. Department of Energy, under contract W-7405-ENG-36 with Los Alamos National Laboratory.

REFERENCES

Bellin, J. L. S., and R. T. Beyer, Experimental investigation of an end-fire array, *J. Acoust. Soc. Am.*, *34*, 1051–1059, 1962.

Birch, F., The velocity of compressional waves in rocks to 10 kilobars, part 1, *J. Geophys. Res.*, *65*, 1083–1102, 1960.

Hiki, Y., and K. Mukai, Ultrasonic three-phonon process in copper crystal, *J. Phys. Soc. Jpn.*, *34*, 454–461, 1973.

Jones, G. L., and D. Kobett, Interaction of elastic waves in an isotropic solid, *J. Acoust. Soc. Am.*, *35*, 5–10, 1963.

Muir, T. G., Nonlinear acoustics: A new dimension in underwater sound, in *Science, Technology, and the Modern Navy, 30th Anniversary 1946–1976*, edited by E. I. Salkovitz, pp. 548–569, Department of the Navy, Office of Naval Research, Arlington, Va., 1976.

Muir, T. G., and J. G. Willette, Parametric acoustic transmitting arrays, *J. Acoust. Soc. Am.*, *52*, 1481–1486, 1972.

Nichols, R. H., Jr., Finite amplitude effects used to improve echosounder, *J. Acoust. Soc. Am.*, *50*, 1086–1087, 1971.

Rolleigh, R. L., Difference frequency pressure within the interaction region of a parametric array, *J. Acoust. Soc. Am.*, *58*, 964–971, 1975.

Taylor, L. H., and F. R. Rollins, Jr., Ultrasonic study of three-phonon interactions, I, Theory, *Phys. Rev., Ser. A*, *136*, 591–596, 1964.

Unterberger, R. R., T. G. Muir, and A. M. Wang, Nonlinear sonar probing of salt, 50th S.E.G. Annual Meeting Technical Program Abstracts, *Geophysics*, *46*, 432, 1981.

Watt, J. P., G. F. Davies, and R. J. O'Connell, The elastic properties of composite materials, *Rev. Geophys.*, *14*, 541–563, 1976.

Welsby, V. G., The non-linear interaction of acoustic waves, in *Underwater Acoustics*, edited by R. W. B. Stephens, pp. 199–216, Wiley-Interscience, New York, 1970.

Westervelt, P. J., Parametric acoustic array, *J. Acoust. Soc. Am.*, *26*, 535–537, 1963.

J. N. Albright, P. A. Johnson, and T. J. Shankland, Earth and Space Sciences Division, Los Alamos National Laboratory, ESS-3:86, MS J979, Los Alamos, NM 87545.

R. J. O'Connell, Department of Earth and Planetary Sciences, Harvard University, Cambridge, MA 02138.

(Received August 22, 1986;
revised November 6, 1986;
accepted January 5, 1987.)